Exploration of the polymorph landscape for 1,1,4,4-tetraphenyl-1,3-butadiene

Exploration of the polymorph landscapefor 1,1,4,4-tetraphenyl-1,3-butadiene

A. Bacchi*,[a]A. Brillante[b], D. Crocco,[a] M. R.Chierotti,[c] R. G. Della Valle,[b] A. Girlando,[a] M. Masino,[a] P. Pelagatti,[a] and E. Venuti[b]

We present a rationalization of the solid state behaviour of 1,1,4,4-tetraphenyl-1,3-butadiene (TPB), a well-known blue luminescent molecule, which retains its emissive properties in the solid state. The crystal structures of four polymorphs and one solvate form are discussed and their relative thermal stability is assessed. The experimental occurrence of the four polymorphs is rationalized on the basis of thermodynamic and kinetic considerations.

Introduction

In the past two decades crystal engineering has become a mature science and a useful tool for material scientists to successfully design materials with desired tailored properties[1]. However, some aspects like understanding crystal nucleation processes and predicting polymorphs still remain very difficult to handle due to the extreme complexity of the chemical physical phenomena at the basis of the birth and growth of a crystal[2]. The problem of polymorph prediction and control is a major focus also for industrial researchers, in particular in the fields of pharmaceuticals, agrochemicals, dyestuffs, explosives and advanced materials[3]. In this paper we present a rationalization of the solid state behaviour of 1,1,4,4-tetraphenyl-1,3-butadiene (TPB)(Figure 1), a well-known blue luminescent molecule, which retains its emissive properties in the solid state[4].

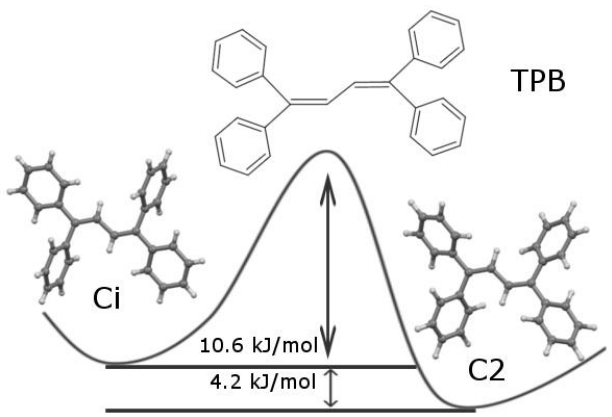

Figure 1. Relative conformer stability for 1,1,4,4-tetraphenyl-1,3-butadiene (TPB).

Many π-conjugated oligomers as oligoacenes, oligophenylenes and oligothiophenes have been extensively studied to obtain a new generation of organic-based devices[5]. Their properties are suitable for use in transistors, light emitting diodes, laser and nonlinear optical devices. Organic semiconductors have several advantages over their inorganic counterparts. They offer the possibility to be solution-processed, allowing the fabrication of devices such as circuits and displays on plastic substrate. They can also be deposited by unconventional methods, such as inkjet and screen printing. Organic semiconductors such as pentacene and rubrenecompete with amorphous Si in performance, and their use as the semiconducting layer in field-effect transistors (FETs) represents another pole of high technological relevance[6]. Although thin films or polymers are the most suitable for the practical use, the optimization of the device performances stimulates the research towards understanding intrinsic properties, a goal that can be achieved through the study of single crystals. However, organic materials present different problems: the chemical purity of the sample, improved by purification techniques, and the polymorphism in the crystalline arrangement. Prior to this publication, TPB was known to occurin three polymorphs, **alpha**[7,8], **beta**[8]and **gamma**[9], whose structural and spectroscopic properties have been extensively discussed[8,10]. In particular, **beta**-TPB shows ASE (amplified spontaneous emission) from the widest crystal face[4], a necessary prerequisite to build a laser. This finding derives from the fact that in the **beta**phasethe lowest energy molecular transition dipole moments are all aligned in a J-type arrangement. The synthesis of the **beta** phase is however not at all straightforward: very small **beta** crystals have been invariably obtained in a mixture with **alpha**crystals.On the other hand, we observe that the **gamma** polymorph is structurally very similar to the **beta** polymorph.

For these reasons,we have decided to undertake a systematic exploration of the polymorph landscape of TPB in order to promote the formation of new phases with possibly favourable alignment of the molecules, and to optimize the procedures to

obtain the **gamma** polymorph in order to compare its properties to those of the elusive **beta** phase. In this paper we will show that new crystalline forms of TPB appeared and that the polymorph landscape is extremely complex.

Table 1. Experimental structures and computed minimum energy structures, with optimized symmetrized geometries, CH bonds at 0.98 Å.The total lattice energy E_{latt} has been corrected for the intramolecularconformation energy E_{mol} = 4.1709 kJ/mol in order to obtain the total energy E_{tot} .Form **delta** contains both conformers, with a 1:3 ratio C*i*: C*2*.

		a(Å)	b(Å)	c(Å)	α(°)	β(°)	γ (°)	V(Å^3)	E_{latt}(kJ/mol)	correction for conformationenergy	E_{tot}(kJ/mol)
alpha	exp	6.259	22.164	7.362	90.	96.349	90.	1014.9			
	calc	6.35274	22.13633	7.17114	90.0000	94.2418	90.0000	1005.689	-148.4	$+E_{mol}$	-144.2
beta	exp	9.736	8.634	24.480	90.	97.11	90.	2041.98			
	calc	9.64072	9.04304	24.57912	90.0000	98.7820	90.0000	2117.721	-137.0	none	-137.0
gamma	exp	9.820	10.110	10.851	99.31	103.64	94.95	1024.38			
	calc	9.72248	9.89436	11.80413	98.5531	108.9155	93.0324	1056.039	-138.9	none	-138.9
delta	exp	9.83500	10.22200	16.06000	83.7900	76.4100	87.9200	1560.054			
	calc	9.76943	10.15342	16.05835	83.1472	76.6186	87.3707	1538.287	-146.6	$+E_{mol}/3$	-145.2

Results and discussion

Crystallization of four polymorphs

TPB crystallizes in different polymorphs which present different molecular conformation and packing. Computation of relative stability shows exceptionally similar packing energies for forms **beta** and **gamma**, and for forms **alpha** and **delta** (Table 1); these values take into account the correction for the molecular conformation energy, that disfavoursstructures containing the C*i* conformer by 4.1709 kJ/mol. With the aim of obtaining new polymorphs and to assess a robust procedure to obtain the **gamma** form, many crystallization experiments have been attempted, using evaporation techniques, gel crystallization, and sublimation; these experiments have led to the discovery of a new polymorph, the **delta** phase, and of a solvate form. The **alpha** polymorph is the commercial form and it has been also the most common product of recrystallization experiments. The **alpha** polymorph has been obtained by crystallization from saturated solutions of hexane, cyclohexanone, pentane, chloroform, ethanol, methanol; it has been also obtained by crystallization from poly(ethylene oxide) (PEO) gels[11] by evaporation, antisolvent liquid diffusion, and counterdiffusion using a variety of solvents (see Supplementary Information). The **alpha** phase was also the crystallization product obtained by sublimation with the cold finger technique. Slurry experiments carried out in dichloromethane at room temperature and at 60°Cstarting respectively from **alpha**, **delta**, and **alpha** seeded with some crystals of **gamma** invariably led to the **alpha** phase.The **beta** polymorph has only be reported once as obtained by physical vapour transport method, but we were not able to reproduce it[8]. The **gamma** polymorph has been obtained only by crystallization from solutions of ethyl-acetate or butyl-acetate, but only in two not reproducible experiments. We obtained the growth of the **gamma** phase also by subliming TPB on the surface of a seed of **gamma**-TPB placed on the wall of a cold finger (Figure S1, Supplementary Information); the nature of the crystals grown on the seed was confirmed by Raman spectroscopy(Figure S2, Supplementary Information). The sublimation of TPB in absence of crystals of **gamma** polymorph led to the crystallization of **alpha**-TPB. The analysis of the DSC diagram of the commercial TPB led to the discovery of the **delta** polymorph: the thermogram showed an exothermic process immediately following the melting of **alpha**-TPB, identified as the crystallization of a higher melting phase, previously unknown (Figure 2). This phase, identified as the new **delta** polymorph, presents a melting point higher than the **alpha** polymorph.

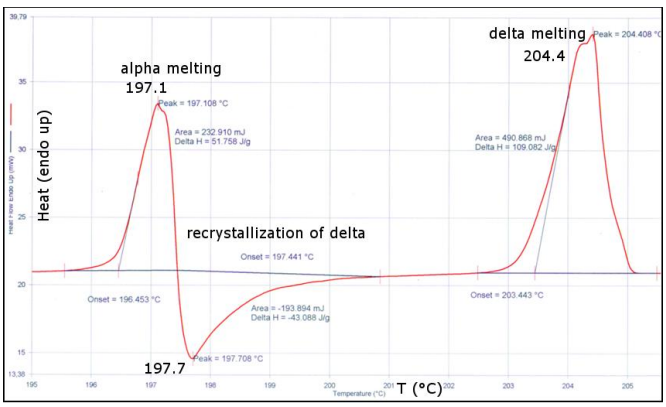

Figure 2. DSC trace for commercial TPB, reported in the range 195-210°C for clarity.

The DSC diagram of the **alpha** phase recrystallized from solution did not show the presence of any contaminant (Figure S3, Supplementary Information). This observation pointed to a seeding by impurities of the **delta** phase present in the commercial TPB. Crystals of the new phase could then be grown by cooling the melt at a cooling rate higher than 0.5° C/min, while cooling at a slower rate produced the **alpha** phase. Table 2 summarizes the outcome of crystallization experiments.

Table 2. Summary of the TPB crystallization experiments outcomes (DCM=dichloromethane).

Alpha	- commercial product - crystallized by slow evaporation from: hexane, cyclohexanone, pentane, chloroform, ethanol, methanol - crystallization from PEO gel (DCM-acetone, DCM-ethanol, DCM-isopropanol, DCM-toluene)

	- sublimation (cold finger) - slow (<0.5°C/min) cooling of the melt - slurry equilibration at 60°C
beta	physical vapour transport (not reproducible)
gamma	- crystallized by evaporation from AcOEt (elusive), AcOBu (elusive) - sublimation on a seed of **gamma**(cold finger)
delta	- fast (> 0.5°C/min) cooling of the melt - recrystallized from the commercial TPB (probably present as seeding impurities)
TPB.c-hex	crystallized by slow evaporation from cyclohexane

Assessment of thermal stability

Crystals of the **beta** phase were not available to us and no thermal data are reported in the original literature[8]. The DSC scan of the pure **alpha**, **gamma** and **delta** polymorphs, recorded at 2°C/min, did not reveal any significant heat exchange prior to melting (Figure S3, Supplementary Information). However, heating a batch of crystals of the **gamma** phase to 170°C and then cooling them back to room temperature with a cooling ramp of 10°C/min resulted in the transition to the **alpha** phase, as shown by following the process by variable temperature Raman spectroscopy (Figure S4, Supplementary Information).

Table 3. Thermodynamic data from DSC experiments for **alpha**, **gamma** and **delta**.

	ΔH_m ($kJmol^{-1}$)	$T_{m(onset)}$ (°C)	ΔS_m ($Jmol^{-1}K^{-1}$)
alpha	40.4	196.4	86.1
gamma	35.4	201.6	74.7
delta	39.1	202.8	82.2

A rationalization of the relative stability of the three experimentally available TPB polymorphs has been attempted by considering the heat of fusion and melting temperatures measured by DSC (Table 3), and the entropy of fusion calculated as $\Delta Sm = \Delta Hm/Tm$. By simple algebra it results that the variation in Gibbs free energy for the transition A>B is given by $\Delta G_{A>B} = (\Delta H_{Am} - \Delta H_{Bm}) - T(\Delta S_{Am} - \Delta S_{Bm})$. By plotting ΔG for the three possible phase transitions **alpha**>**delta**, **alpha**>**gamma** and **delta**>**gamma** as a function of temperature (Figure S5, Supplementary Information), a tentative picture of the relative phase stability can be gained (Figure 3), with the caveat that transition temperatures are just rough estimates and must be taken as indicative values. In fact both the calculated energy differences at zero kelvin (Table 1) and the measured melting enthalpies (Table 3) point to an extremely elusive system, where the polymorph stability within the pairs alpha/delta (1 kJ/mol computed difference, 1.3 kJ/mol melting difference) and beta/gamma (1.3 kJ/mol computed, melting difference being not available) is practically similar.

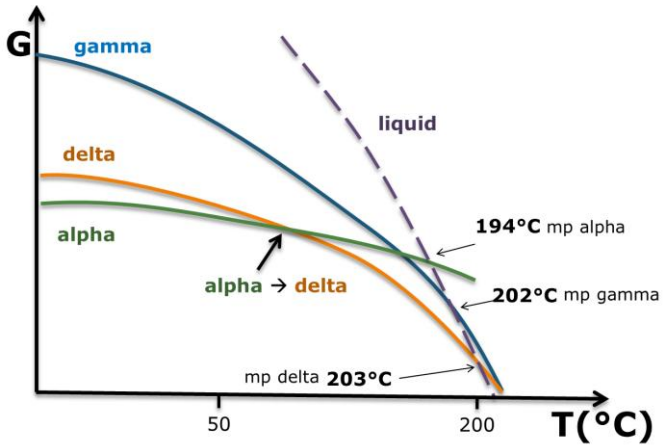

Figure 3. Proposed picture of the relative stability of TPB polymorphs **alpha**, **gamma** and **delta** in the temperature range from RT to the melting points.

The **alpha** polymorph is the thermodynamically stable form at room temperature (RT), up to a tentative temperature of about 63°C, where the **delta** form becomes more stable in an enantiotropic relationship (Figure S5, Supplementary Information), although the transition is not detected by the DSC scan at 1, 2, 10 and 20°C/min (Figure S3, Supplementary Information). The**gamma** phase is always metastable referring to the most stable form in all the temperature range, even if it is related to the **alpha** phase by an enantiotropic transition occurring at around a tentative temperature of 160°C, where **alpha** is metastable with respect to **delta**. This picture justifies the order of the melting points (Tm **alpha**<**gamma**<**delta**), the fact that up to a tentative temperature of around63°C the **alpha** phase is the most stable, as indicated by the slurry experiments, and the conversion between **gamma** and **alpha** observed on cooling a batch of **gamma** crystals down from 170°C to RT. Finally, the RT thermodynamically favoured **alpha** phase may be obtained from the melt when the cooling rate is very slow, otherwise the **delta** form, initially more stable at high temperature, is kinetically frozen to RT by a cooling faster than 0.5°C/min.Attempts were made to detect the conversion form alpha to delta expected tentatively at about 63°C by DSC measurements at different scan rates, but no evidence of thermal exchange has been detected (Figure S3, Supplementary Information). A sample of commercial alpha-TPB has also been heated and stored for 3 hours at 140°C in order to allow the expected phase transition, but the XRPD trace revealed no change in the powder (Figure S10, Supplementary Information).The absence of phase transitions in these experiments of the three polymorphs can be reasonably ascribed to slow kinetics for the conversions.

Structural rationalization

TPB is a relatively rigid molecule with just four torsional degrees of freedom around the single bonds carrying the phenyl groups. Taking into account rotation of phenyl groups around single bonds, two ideal stable conformations exist, with C_i and C_2 point group symmetry respectively, that may convert through a C_{2h} planar high energy conformer (Figure 1). The C_2 conformer is more stable than the C_i one by 4.2 kJ/mol, and the energetic barrier for the interconversion requires 10.6 kJ/mol. TPB adopts an approximate C_i conformation in the **alpha**

phase, and an approximate C_2 conformation in the **beta** and **gamma** phases.
Computed lattice energies at the minima, corrected for intra-molecular conformational energy show that **alpha** is more stable (Table 1) than **beta** and **gamma** polymorphs, which in turn are almost isoenergetic. In fact the crystal packing of the **beta** and **gamma** polymorphs are rather similar (Figure 4): both phases are characterized by ribbons consisting in double rows of molecules with identical arrangement, that are then aligned with different shifts in the two polymorphs.

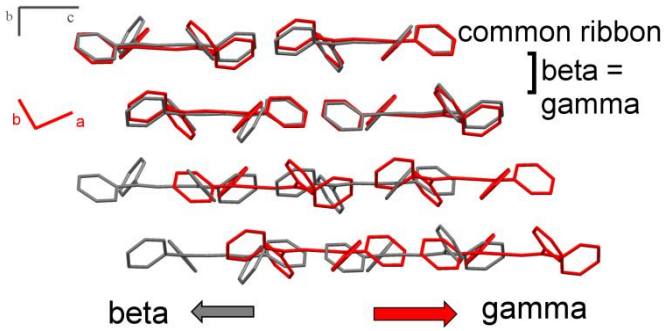

Figure 4. Comparison of the crystalline arrangement in the **beta** (grey) and **gamma** (red) polymorphs, showing the existence of a common motif identical in the two crystal packings.

From a purely geometrical point of view, the shortest intermolecular contacts are obviously the same for **beta** and **gamma** within the common ribbons, consisting of CH···pi interactions involving both the aryl and the olefinic double bonds. The association of the ribbons is also based on essentially similar aryl···aryl edge-to-face interactions in both polymorphs, even if the molecules involved in the contacts are differently related each other. By inspection of the energy related to intermolecular association, the three strongest interactions in the two polymorphs, identified by computing the inter-molecular potentials with the atom-atom potentials method using the UNI force field [12,13], are essentially identical in the two structures (Figure 5). This confirms that although differently shifted, the energetic difference between the arrangement of the ribbon motif in **beta**- and **gamma**-TPB are elusive and that a rational method for the selective isolation of the two is not readily predictable neither on the basis of structural nor of thermodynamic considerations. On the other hand, in **alpha**-TPB the molecules are disposed in a herringbone pattern, which actually yields a tighter packing[8]. Nevertheless, the three strongest intermolecular interactions found in the crystal packing of **alpha**-TPB are actually weaker than those observed in the two other polymorphs, even if the total packing energy for **alpha** is the most stabilizing. This points to a kinetic advantage for the formation of the less stable **beta**- and **gamma**-TPB phase, that can cluster together more favourably the first neighbouring molecules, thus justifying the occasional occurrence of the metastable **gamma** form in a modest number of crystallization experiments.

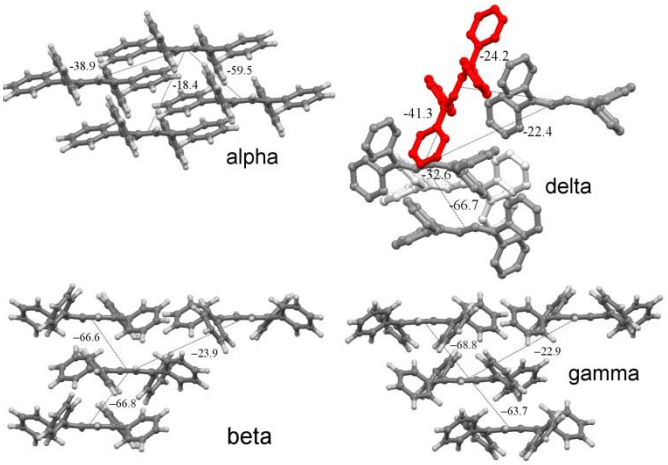

Figure 5. Strongest intermolecular interactions (kJ/mol) between the nearest neighbouring molecules for the four TPB polymorphs. The Ci conformer in **delta** is indicated in red.

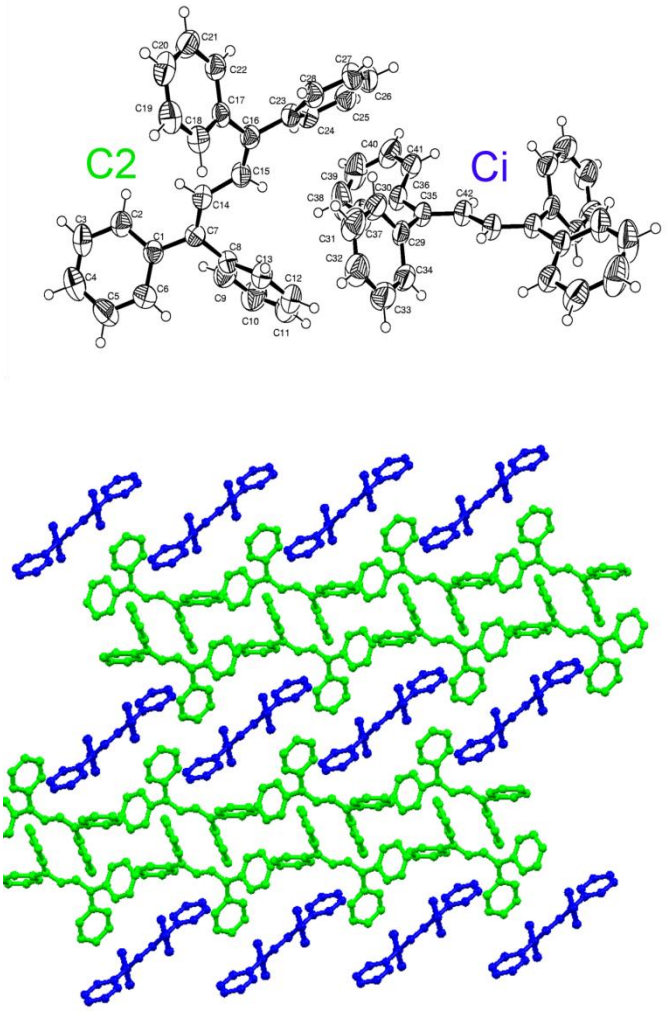

Figure 6. Molecular conformations (top) and crystal packing (bottom) of the new delta-TPB polymorph. The C_2 conformer is represented in green, the Ci conformer is blue.

The crystal structure of the newly discovered **delta** polymorph contains both conformers C_2 and C_i, the latter sitting on a crystallographic centre of symmetry (Z'=1.5) (Figure 6). The computed lattice energies (Table 1) show that the **delta** and the **alpha** polymorphs are practically equally stable; on the other hand the strongest interaction between the nearest neighbouring molecules is the same as in the **beta** and the **gamma** polymorphs. Most interestingly, the C_2 molecules of **delta** are aligned in a supramolecular ribbon identical to the arrangement of the **gamma** form, with the C_i molecules flanking this motif (Figure 6). By examining the three polymorphs containing C2 molecules, i.e. **beta**, **gamma** and **delta**, it is possible to identify a tetramolecular cluster conserved in all these structures (Figure 7); this could be considered a sort of structural invariant and includes the strongest nearest neighbours interactionshown in Figure 5. It is worth noting that the cluster, made up of two parallel couples of aligned molecules, presents the advantageous J-type aggregation of the TPB transition dipole moments[5],and is present in all polymorphs, except the **alpha** one.Notably, **beta**, **gamma** and **delta** phases are exclusively obtained from physical vapour transport (**beta**),seeded sublimation(**gamma)** or from the melt (**delta**), while **alpha** form is the prominent product from solution crystallization. Combining the results of packing energy calculations shown in Table 1 and the consideration on the energy of closest contacts reported in Figure 5, it can be envisaged that the most stable C2 conformer, present in the melt or in the gas phase, quickly assemble by the most stabilizing arrangement observed in Figure 7, and allow the nucleation of **beta**, **gamma** or **delta**; on the other hand, solvent mediation allows the metastable conformer Ci to choose the most favourable long range stabilization that ultimately favours the global energy minimum constituted by the alpha phase. NMR solution experiments were performedtoinvestigate the existence of supramolecular assemblies in solution; unfortunately, attempts made to detect these tetramolecular clusters in solution by ^{1}HNMR spectroscopy failed. In fact, the spectra of TPB recorded in deuterated dmso at different concentrations were always superimposable (Figure S11, Supplementary Information).

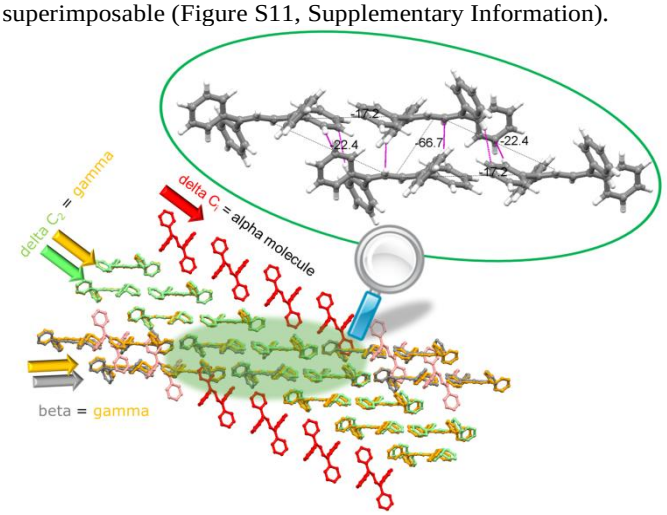

Figure 7. Superimposition of the crystal packing of **beta** (grey), **gamma** (yellow) and **delta** (green=C_2 conformer, red=C_i conformer) shows a highly conserved tetramolecular cluster (shadowed in green and magnified in the inset). Strongest intermolecular interactions (kJ/mol) are reported, and shortest CH…pi contacts are highlighted in pink.

Regarding the **alpha** form, the most important interactions governing the crystal formation can be inferred by observing that this polymorph occurs persistently in a needle morphology, no matter the crystallization procedure. Crystal faces were indexed showing that the needles are elongated along the (100) directions (Figure S6, Supplementary Information) hinting that the most relevant interactions for the process of crystal growth for **alpha** in fact coincide with the strongest nearest neighbours interactions evidenced by intermolecular potential energy calculations[14,15] (E=-59.5 kJ/mol in Figure 5).

Solvate form

Crystallization of TPB from cyclohexane afforded a solvated phase **TPB.c-hex**, where the TPB molecule adopts an exact crystallographic Ci conformation. Cyclohexane is hosted in channels (Figure 8) and easily escapes: crystals rapidly deteriorate when extracted from the mother liquor. Cyclohexane can be replaced in the channels by cyclohexanone by a solid-gas process by simply exposing a freshly prepared powder of **TPB.c-hex** to vapours of cyclohexanone; the exchange is complete in 15 minutes as shown by the IR spectrum recorded during the process (Figure S7, Supporting Information). It is known that sometimes solvent removal from a solvate phase may be the only route to obtain some particularly elusive polymorph forms[16].

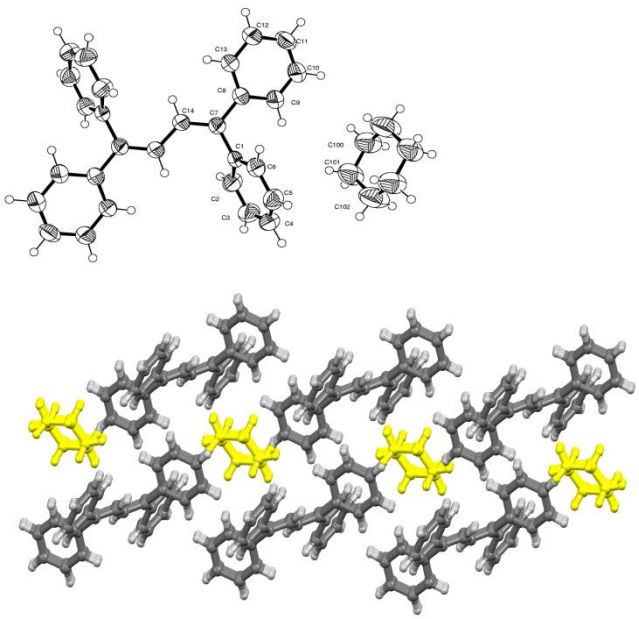

Figure 8. Top: molecular structure and labelling of **TPB.c-hex**. Bottom: crystal packing, evidencing that cyclohexane (yellow) is arranged into channels.

The process of solvent loss for **TPB.c-hex** was monitored by ^{13}C CPMAS solid-state (SS) NMR in order to identify the unsolvated phase formed by guest removal. The spectra are reported in Figure 9 together with that of **alpha** and **delta** for comparison. The spectrum of **gamma** could not be acquired due to the small amount of the sample. The spectra are characterized by to groups of peaks around 128 and 142 ppm. These are assigned to the CH groups (both aromatic and olefinic) and to the quaternary carbon atoms (both aromatic and olefinic), respectively. Although **delta** contains Ci molecules

presenting the same packing of **alpha**, the spectra are very different concerning the resonances due to the quaternary carbon atoms. This can be due either to the presence of a olefinic-aryl CH···pi interaction in **delta** only and to the overall packing effect. The **TPB.c-hex** spectrum also shows the cyclohexane signal (at 27.6 ppm) whose intensity, however, is much lower than expected indicating the spontaneous and sudden release of the guest. By monitoring the desolvation process **TPB.c-hex** of at different times (desovated T0=2 hours and desolvated T1=1 week), an unknown transient phase is present before the powder converts to the stable **alpha** polymorph. On passing from desolvated T0 to desolvated T1, the cyclohexane peak (insets in Figure 9) decreases in intensity confirming that the structure rearrangement occurs through solvent loss. Unfortunately, the strong signal overlapping prevents any further characterization of the intermediate phase.

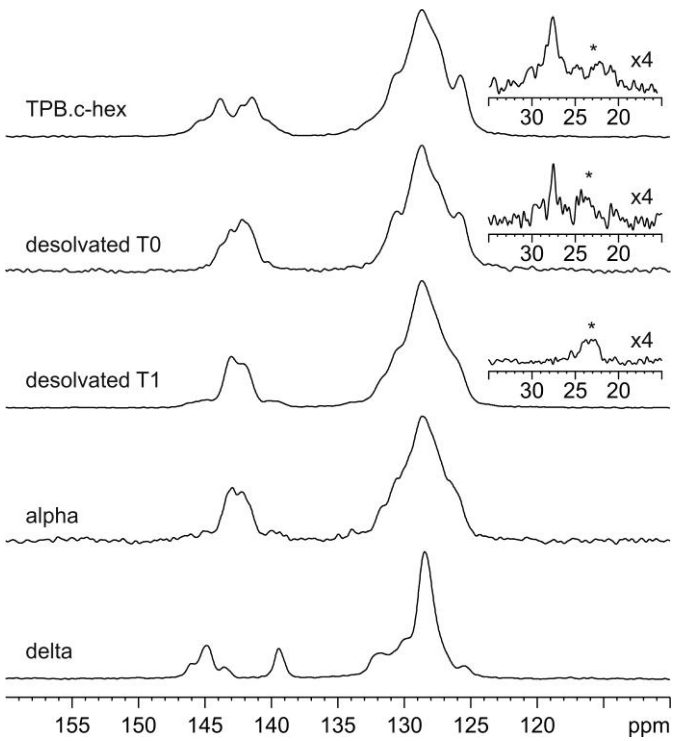

Figure 9. ^{13}C (100.64 MHz) CPMAS SSNMR spectra of **TPB.c-hex** and its desolvated forms (desolvated T0 and T1) together with that of **alpha** and **delta**. All spectra are recorded with a spin rate of 12 kHz. Insets report the aliphatic region of the spectrum

Experimental

Crystallization

TPB was purchased from Sigma-Aldrich and used as received; the melting point indicated on the label corresponds to the **alpha** form. The **alpha** phase is obtained by crystallization from a saturated solution in different solvents: hexane, cyclohexanone, pentane, chloroform, ethanol, methanol. The following general procedure was followed: about 30 mg of TPB were dissolved in ca. 4 mL of the respective solvent, filtered, and kept for slow evaporation at room temperature. Single crystals were obtained over a period from two days to a fortnight. The **alpha** phase was also always obtained by crystallization in PEO(poly(ethylene) oxide) gel(MW 600000 Da). PEO gel was used since TPB is not soluble in water. Different PEO concentrations were used in order to optimize gel preparation. The following general procedure was used: 1 ml of solvent was added to the appropriate amount of PEO (50-100 mg) to attain the desired concentration in a 2 ml screw-capped vial. The mixture was then stirred until a homogeneous solution was obtained. The experiments were carried out at 298 K. In those cases where dissolution was not achieved, the mixture was heated to 313 K until dissolution was observed. The solution was then left undisturbed at 298 K until the formation of a gel. The gels were prepared using a single solvent or solvent mixtures: in the first case the solvents used were acetonitrile, benzonitrile, chloroform, dichloromethane, acetone. The solvent mixtures used were dichloromethane (DCM)-acetone, DCM-ethanol, DCM-isopropanol, DCM-toluene. Crystals of the **alpha** polymorph were invariably obtained, all with needle morphology with the exception of the gel prepared in acetonitrile, where irregular prisms were obtained. We noticed that often the needles are bent (Figure S8, Supplementary Information). The **gamma** phase was obtained only twice by crystallization form a saturated solution of ethyl acetate and from one of butyl acetate respectively. TPB was dissolved in ca. 4 mL of solvent, filtered, and kept for slow evaporation at room temperature. Single crystals were obtained over a period from fifteen days to two months. Unfortunately with this method, the **gamma** phase is not reproducible and attempts to obtain it by the same methods afforded the **alpha** polymorph. Sublimation experiments were carried out with the cold finger method, always giving **alpha** crystals; when crystals of TPB were sublimated in presence of seeds of the gamma phase glued to the cold finger, microcrystals of **gamma** were reproducibly formed on the surface of the seed, while the **alpha** polymorph crystallized on the walls of the cold finger.

DSC measurements

Thermal analyses were carried out with on a Mettler Toledo DSC 821e instrument. The working conditions were as follows: gas flow, N_2 at 25 ml/min; heating rate from 1°C/min to 20°C/min; closed and vented sample aluminium pan; sample weights ranging between 2.200 and 3.000 mg.

X-ray single crystal diffraction

Single crystal X-ray diffraction data were collected using the Mo Kα radiation (λ = 0.71073 Å) on a SMART APEX2 diffractometer at room temperature (293K). The collected intensities were corrected for Lorentz and polarization factors and empirically for absorption by using the SADABS program[17]. Structures were solved by direct methods using SIR97[18] and refined by full-matrix least-squares on all F^2 using SHELXL97[19] implemented in the WinGX[20] package. Hydrogen atoms were introduced in calculated positions. Anisotropic displacement parameters were refined for all non-hydrogen atoms. Hydrogen bonds have been analysed with SHELXL97[19] and PARST97[21] and extensive use was made of the Cambridge Crystallographic Data Centre packages for the analysis of crystal packing[22]. Table 4 summarizes crystal data and structure determination results.
Intermolecular potentials between nearest neighbouring molecules were estimated by using the UNI Force Field[12,13] implemented in Mercury.

X-ray powder diffraction

Powder XRD analyses were collected using Cu K_α radiation with a Thermo ARL X'TRA powder diffractometer equipped with a Thermo Electron solid state detector. In order to investigate possible phase transition of commercial alpha, a diffraction pattern of commercial alpha was measured at room temperature; then the sample was heated and kept at 140°C for 3 hours, and the diffraction pattern was measured again.

Solution ^{1}H NMR Spectroscopy

^{1}HNMR spectra were recorded on a Bruker AV300 at 27°C. The chemical shift values are referred to TMS. The concentrations of the solutions varied from 4 mM to 60 mM.DMSO was preferred to CDCl3 since it brings to a higher resolution of the aromatic region thus allowing a closer inspection/comparison of the signals

SSNMR Spectroscopy

SSNMR measurements were made on a Bruker AVANCE II 400 instrument operating at 400.23 and 100.65 MHz for ^{1}H and ^{13}C, respectively. Spectra were recorded at RT at the spinning speed of 12 kHz. Cylindrical 4-mm outer diameter (O. D.) zirconia rotors with sample volume of 80 μL were employed. For ^{13}C CPMAS experiments, a ramp cross polarization pulse sequence was used with contact times of 3.5 ms, a ^{1}H 90° pulse of 4 μs, recycle delays from 5 to 80 s, and 60 transients. The two-pulse phase modulation (TPPM) decoupling scheme was used with a frequency field of 75 kHz. The ^{13}C scale was calibrated indirectly to glycine (^{13}C methylene signal at 43.86 ppm) as external standards.

Raman measurements

Raman spectra have been measured using the 647 nm excitation line from a Kr^+ laser (laser power 2-3 mW at the sample). The scattered radiation was then analyzed by a Renishaw 1000 microspectrometer (2 cm^{-1} spectral resolution) equipped with a long-pass edge filter. High temperature experiments have been obtained placing the sample on a Linkam hot stage fitted under the microscope.

It is well known that Raman spectroscopy represents a fast and reliable tool for polymorph identification, since low-frequency Raman spectra characterize the lattice (inter-molecular) phonons, which are the most sensitive to the different crystalline packing[6]. In the case of TPB polymorphs, however, TPB molecules assume different molecular conformations, resulting in spectral differences between polymorphs even in the easily accessible region of the intra-molecular vibrations. By carefully analyzing the spectra, we have identified as the most diagnostic spectral region the 700-1000 cm^{-1}, where the CH bending modes of the phenyl groups occur (Figure S2, Supplementary Information). In this diagnostic region, the band pattern of the beta and gamma polymorphs, where TPB has approximate C_2 symmetry, is very similar and clearly different from that of the alpha polymorph. On the other hand, delta-TPB band pattern is a sort of superposition of those of the other polymorphs, reflecting the fact that both molecular conformers cocrystallize in this polymorph.

Computational methods

Standard Density Functional Theory (DFT) methods have been employed for isolated TPB in the different conformations (B3LYP exchange correlation functional, 6-31G(d) basis set.). For the calculations of the energies of the crystallinestructures we started from the experimental X-ray data and located the minimumof an empirical potential, represented by anatom–atom Buckingham model plus a Coulomb term[23]. Corrections for the intra-molecular energies of the different conformers have been introduced.

Table 4. Crystal data and structure refinement for **TPB.c-hex** and **delta**.

	TPB.c-hex	**delta**
Empirical formula	C_{34} H_{34}	C_{28} H_{22}
Formula weight	442.6	358.46
Temperature	293(2) K	293(2) K
Wavelength	0.71073 Å	0.71073 Å
Crystal system, space group	triclinic, P-1	triclinic, P-1
Unit cell dimensions	a = 8.846(3) Å α = 74.927(6) ° b = 8.839(3) Å β = 64.092(5) ° c = 10.016(3) Å γ = 68.128(6) °	a = 9.835(7) A α = 83.79(1)° b = 10.222(7) A β = 76.41(1)° c = 16.06(1) A γ= 87.92(1)°
Volume	649.3 (4) $Å^3$	1560.1(18) $Å^3$
Z, Calculated density	1, 1.13 Mg/m^3	3, 1.14 Mg/ m^3
Absorption coefficient	0.063 mm^{-1}	0.065 mm^{-1}
F(000)	238	570
Theta range for data collection	2.28° to 26.34°	1.31° to 23.42°
Reflections collected / unique	5164 / 2622 [R(int) = 0.0581]	14226 / 4516 [R(int) = 0.0523]
Refinement method	Full-matrix least-squares on F^2	Full-matrix least-squares on F^2
Data / restraints / parameters	2622 / 0 / 198	4516 / 0 / 379
Goodness-of-fit on F^2	0.976	1.039
Final R indices [I>2sigma(I)]	R_1 = 0.0677, wR_2 = 0.1950	R1 = 0.0582, wR2 = 0.1614
R indices (all data)	R_1 = 0.1203, wR_2 = 0.2321	R1 = 0.0782, wR2 = 0.1822
Largest ΔFmax/min	0.36/ -0.21e·$Å^{-3}$	0.25 / -0.23 e. $Å^{-3}$

Conclusions

A careful characterization of the solid-state behaviour of TPB is important since so far the solid-state properties of this molecule have been poorly investigated, at least until it has been shown that one particular polymorph exhibits amplified spontaneous emission (ASE), and could therefore be used for building a laser[9].

In this work we show that the polymorph landscape of TPB is complex and elusive mostly because the interactions involved in the stabilization of the polymorphs are quite weak and poorly directional. From this work it is clear that the **alpha** polymorph is the thermodynamically stable phase at ambient conditions and that it is persistently obtained in most of the crystallization experiments. On the other hand, in the narrow T range 200-204°C it is easy to obtain the previously unknown **delta** polymorph from the melt, that can easily be quenched at room temperature. The **gamma** form is highly elusive, and the best way to obtain it is by sublimation of TPB on a seed; however, the morphology of these tiny crystals did not allow to perform measurements suitable to compare its optical properties to the ones observed for the **beta** phase. From a structural point of view, it is interesting to notice that a highly conserved molecular cluster, with a favourable arrangement of TPB molecules, constitutes the core of all the polymorphs containing the C_2 conformer. A solvate form was also obtained during polymorph screening; it rapidly deteriorates when extracted from the mother liquor and the ^{13}C-CPMAS SSNMR analysis of the process hinted for the presence of other polymorphs not structurally characterized so far. A last observation is worth of note: the commercial crystalline TPB, described as the **alpha** form according to the melting point reported on the label, was contaminated by seeds of the **delta** polymorph, not detectable by XRPD. The presence of polymorphic impurities is normally not an issue considered for commercial products; in our case led to the discovery of a new phase, in other cases it could lead to alteration of results for measures sensitive to crystal structure such as spectroscopic investigations in the solid state.

Acknowledgements

The Laboratorio di Strutturistica 'Mario Nardelli' of the Dipartimento di Chimica at the University of Parma is gratefully acknowledged for providing diffraction facilities. This work has been supported by the Italian Ministry ofUniversity and Research (M.I.U.R.) under the project PRIN-2010ERFKXL.

Notes and references

[a] Department of Chemistry, University of Parma, Parco Area Scienze 17/A, 43124 Parma, Italy

[b] Dipartimento di Chimica Industriale 'Toso Montanari' and INSTM-UdR Bologna, Bologna University, I-40136, Bologna, Italy

[c] Department of Chemistry and NIS, University of Torino, Via P. Giuria 7, 10125 Torino, Italy.

† CCDC 990581-990582. Electronic Supplementary Information (ESI) available: [details of any supplementary information available should be included here].

[1] G.R. Desiraju, *J. Am. Chem. Soc*., 2013, **135**, 9952

[2] R. J. Davey, K. Allen, N.Blagden, W. I. Cross, H. F. Lieberman, M. J. Quayle, S.Righini, L. Seton, G. J. T.Tiddy, *CrystEngComm* . 2002, **4**, 257

[3] J. Bernstein, *Polymorphism in Molecular Crystals*, Oxford University Press, New York, 2008;

[4] S. Tavazzi, L. Silvestri, L. Miozzo, A. Papagni, P. Spearman, S. Ianelli, A. Girlando, A. Camposeo, M. Polo and D. Pisignano, *ChemPhysChem*. 2010, **11**, 429

[5] M. Lefenfeld, G. Blanchet and J.A. Rogers, *Adv. Mater*. 2003, **15**, 1188 ; H. E. A. Huitema, G. H. Gelinck, J. B. P. H. van der Putten, K. E. Kuijk, C. M. Hart, E. Cantatore, P. T. Herwig, A. J. J. M. van Breemen and D. M. de Leeuw, *Nature*. 2001, **414**, 599

[6] A. Brillante, I. Bilotti, R.G. Della Valle, E. Venuti and A. Girlando. *CrystEngComm*. 2008, **10**, 937

[7] K. Baba, H. Kasai, S. Okada, H. Oikawa and H. Nakanishi, *Opt. Mater*. 2002, **21**, 591

[8] A. Girlando, S. Ianelli, I. Bilotti, A. Brillante, R. G. Della Valle, E. Venuti, M.Campione, S. Mora, L. Silvestri, P. Spearman and S. Tavazzi. *Crystal Growth & Design* 2010, **10**, 2752; S. Mora, S. Tavazzi, and P. Spearman, *Synthetic metals*, 2012, **162**, 1737

[9] I. Ino, L. P. Wu, M. Munakata, T. Kuroda-Sowa, M. Maekawa, Y. Suenaga and R. Sakai, *Inorg. Chem*. 2000, **39**, 5430.

[10] A. Bacchi, I. Bilotti, A. Brillante, D. Crocco, R. G. Della Valle, A. Girlando, M. Masino, P. Pelagatti and E. Venuti, *J. Ram. Spectr*., 2013, **44**, 905

[11] L. Carlucci, G. Ciani, J. M. Garcia Ruiz, M. Moret, D. M., Proserpio and S. Rizzato, *Cryst. Growth Des*. 2009, **9**, 5024

[12] A. Gavezzotti, *Acc. Chem. Res*., 1994, **27** 309

[13] A. Gavezzotti and G. Filippini*J. Phys. Chem*., 1994, **98**, 4831

[14] A. Bacchi, G. Cantoni, D. Cremona, P. Pelagatti, and F. Ugozzoli, *Angew. Chem. Int. Ed.* 2011, **50**, 3198

[15] G. M. Lombardo, A. Rescifina, U. Chiacchio, A. Bacchi and F. Punzo, *Acta Crystall. Sect. B*, 2014, **B70**, 172

[16] J. Bernstein, *Polymorphism in Molecular Crystals*, Oxford University Press, New York, 2008

[17] SAINT, SAX, Area Detector Integration, Siemens Analytical instruments Inc., Madison, Wisconsin, USA; G. Sheldrick, SADABS, Siemens Area Detector Absorption Correction Software, University of Goettingen, Germany, 1996.

[18] M. C. Burla, R. Caliandro, M. Camalli, B. Carrozzini, G. L. Cascarano, L. De Caro, C. Giacovazzo, G. Polidori and R. Spagna, *J. Appl. Cryst*. 2005, **38**, 381

[19] G. Sheldrick, Shelxl97, Program for structure refinement, University of Goettingen, Germany, 1997

[20] L. J. Farrugia, *J. Appl. Crystallogr*., 1999, **32**, 837

[21] M. Nardelli, *J. Appl. Crystallogr*., 1995, **28**, 659

[22] I. J. Bruno, J. C. Cole, P. R. Edgington, M. Kessler, C. F. Macrae, P. McCabe, J. Pearson and R. Taylor, *ActaCryst. Sect B*, 2002, **B58**, 389; C. F. Macrae, I. J. Bruno, J. A. Chisholm, P. R. Edgington, P. McCabe, E. Pidcock, L. Rodriguez-Monge, R. Taylor, J. van de Streek and P. A. Wood, *J. Appl. Cryst*. 2008, **41**, 466

[23] A. Girlando, L. Grisanti, M. Masino, I. Bilotti, A. Brillante, R. G. Della Valle,E. Venuti. *Phys.Rev. B* 2010; **82**, 035208

Supporting Information

Exploration of polymorph landscape for 1,1,4,4-tetraphenyl-1,3-butadiene

A. Bacchi*,[a]A. Brillante[b], D. Crocco,[a] M.R.Chierotti,[c]R. G.Della Valle,[b] A. Girlando,[a]M. Masino,[a]P. Pelagatti,[a] and E. Venuti[b]

[a] Department of Chemistry, University of Parma, Parco Area Scienze 17/A, 43124 Parma, Italy

[b] Dipartimento di Chimica Industriale 'Toso Montanari' and INSTM-UdR

Bologna, Bologna University, I-40136, Bologna, Italy

[c] Department of Chemistry and NIS, University of Torino, Via P. Giuria 7, 10125 Torino, Italy.

We present a rationalization of the solid state behaviour of 1,1,4,4-tetraphenyl-1,3-butadiene (TPB), a well-known blue luminescent molecule, which retains its emissive properties in the solid state. The crystal structures of four polymorphs and one solvate form are discussed and their relative thermal stability is assessed. The experimental occurrence of the four polymorphs is rationalized on the basis of thermodynamic and kinetic considerations

Solvent	
Toluene	TOL
Nitromethane	NME
Water	H2O
Heptane	HEP
Acetonitrile	ACN
2-Propanol	ISP
1,2-Dichloroethane	DCE
Benzene	BZN
Butanone	BNA
Ethanol	EOH
Ethyl Acetate	ETA
n-Hexane	HEX
Ciclhoexane	CHEX
Methanolo	MET
Tetrahyidrofuran	THF
Chloroform	CLF
Acetone	ACE
Dichloromehtane	DCM
n-Pentane	PEN

Legend for solvent labels

Table S1. Crystallization form PEO gel

- **doped PEO gel**

A supersaturated solution of TPB in 1ml solvent was microfiltered and 50 mg of PEO were added under stirring. The solution was allowed to stand in a closed vial. G indicates the formation of the gel, F indicates the formation of the floccules and I that the PEO is insoluble; whereas r.t indicates that the experiments were conducted at room temperature.

SOLVENTS	T	OUTCOME	NOTES
DCM	r.t.	Around 3 days Morfology: needles α phase	G
ACN	r.t.	Around 45 days Morfology: prismatic α phase	G
NME	r.t.	Around 3 days Morfology: needles α phase	G
CLF	r.t.	Around 20 days Morfology: needles α phase	G
DCM/EOH (1:1)	r.t.		F
DCM/EOH (4:1)	r.t.		F
DCM/EOH (1:4)	r.t.	Around 3 days Morfology: needles α phase.	F
DCM/THF (1:1)	r.t.	-	G
DCM/THF (4:1)	r.t.	-	G
DCM/THF (1:4)	r.t.	-	F
DCM/BNA (1:1)	313 K	Around 4 hours Morfology: needles α phase.	G

DCM/ETA (1:1)	r.t.	-	F
DCM/MET (1:1)	r.t.	-	F
DCM/ISP (1:1)	r.t.	-	G
DCM/TOL (1:1)	r.t.	-	G

- **counterdiffusion**

Crystallizations were carried out in a glass U-tube. A gel was prepared in DCM and inserted in the middle section of the tube, a saturated solution of TPB was added in the chosen solvent on the one hand and on the other the anti-solvent

SOLVENT/ANTISOLVENT	T	OUTCOME	NOTES
DCM/hexane	r.t.	Around 20 gg Morfology: needles α phase.	G
DCM/ISP	r.t.	Around 20 gg Morfology: needles α phase.	G

Figure S1. SEM image of gamma crystals grown by sublimation on a gamma seed

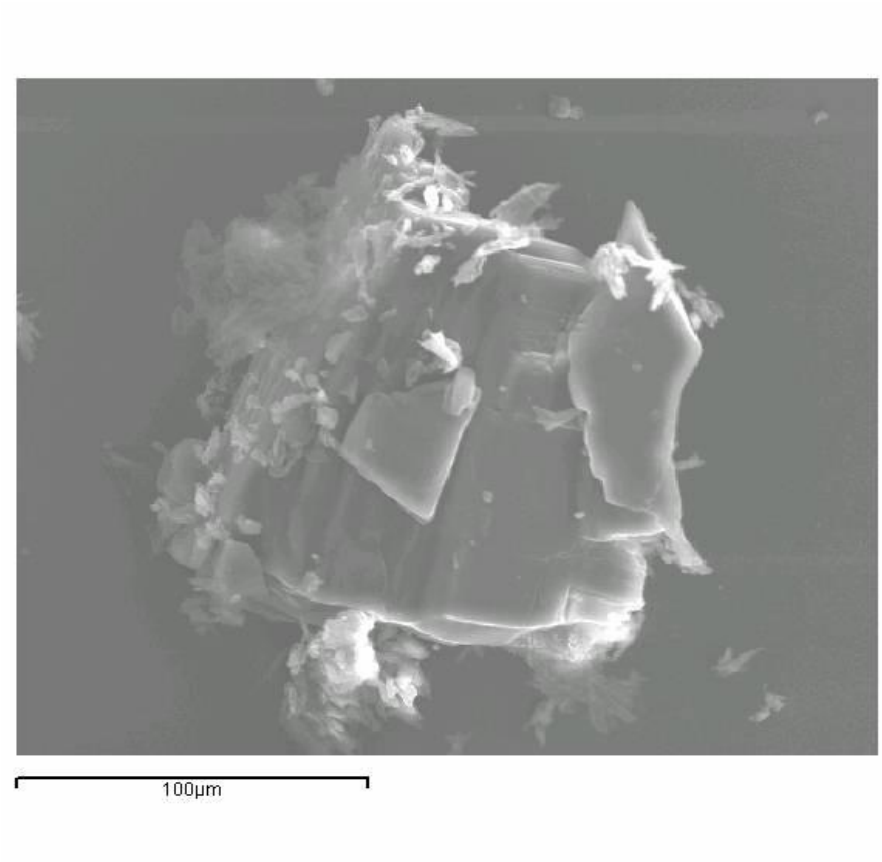

Figure S2. Unpolarized Raman spectra of the four polymorphs of TPB in the high-frequency diagnostic spectral region

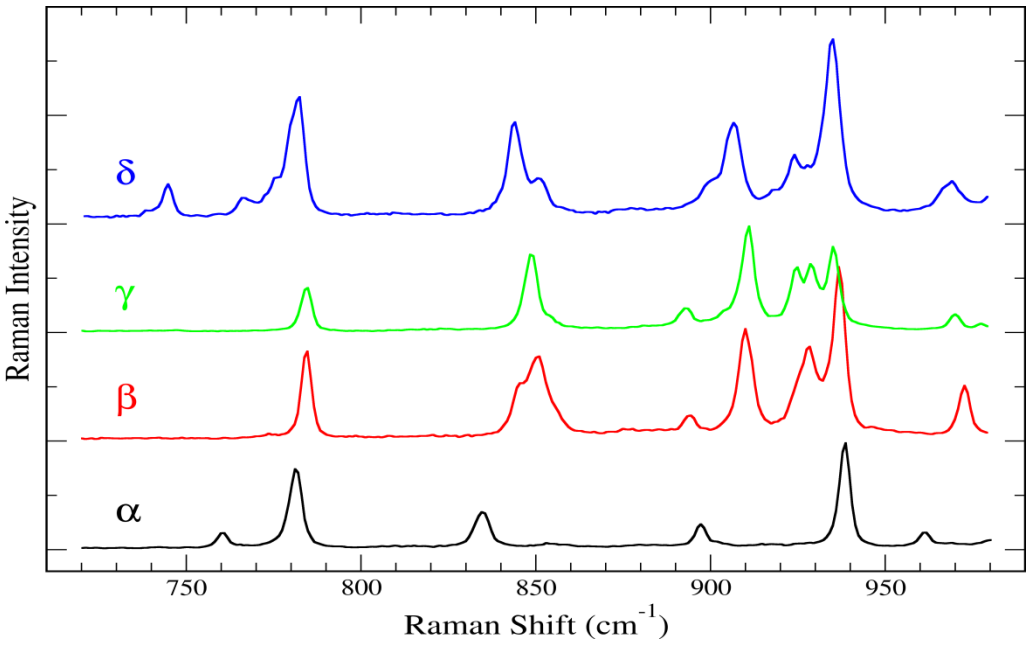

Figure S3. DSC experiments for alpha (as received), alpha (recrystallized), gamma, delta polymorphs. The heat of fusion for the delta polymorph has been measured from the transition observed in the first diagram (see Figure 2 in the manuscript), since the sample weight in the measure on pure delta was unreliable.The vertical steps in the baselines are the predicted consequence of a change of heating rate from 10°C/min to 2°C/min; the scan has been slowed down to better detect the melting temperature.The endothermic phenomenum marked by an arrow on the DSC trace of the gamma phase is attributed to impurities, that are reported to possibly contaminate commercial TPB.

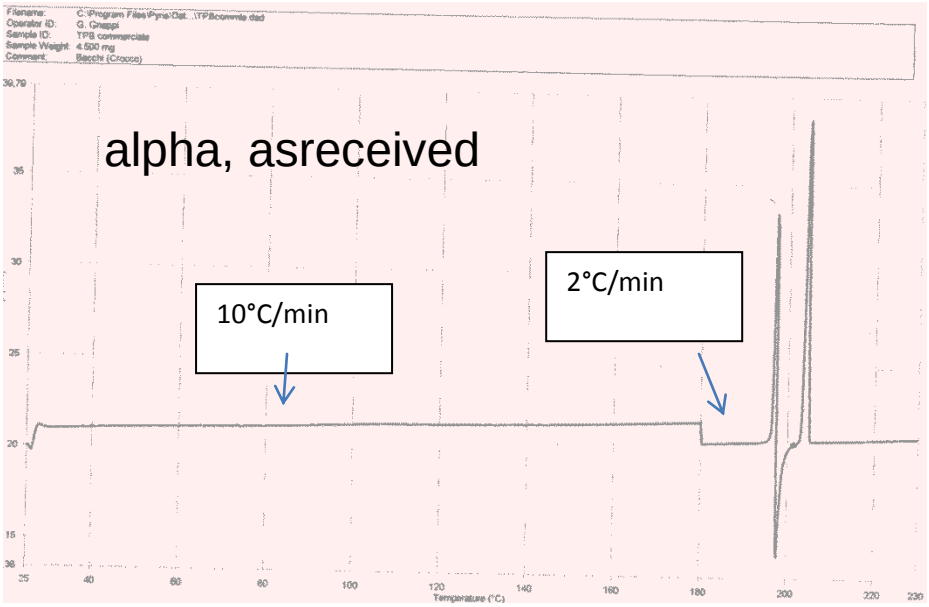

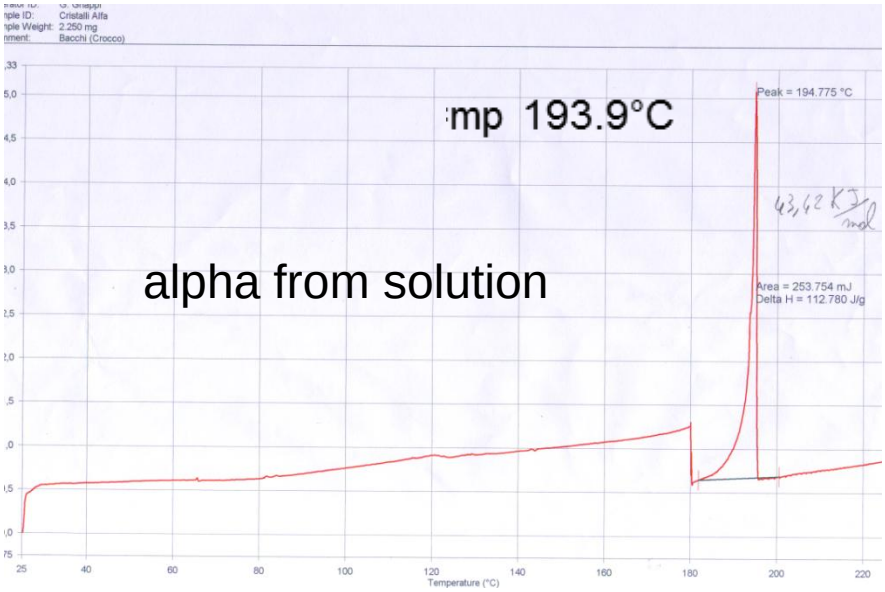

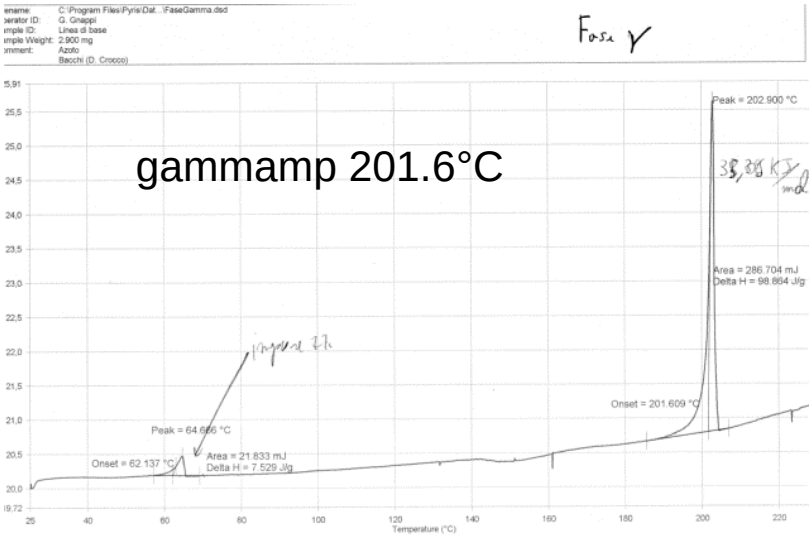

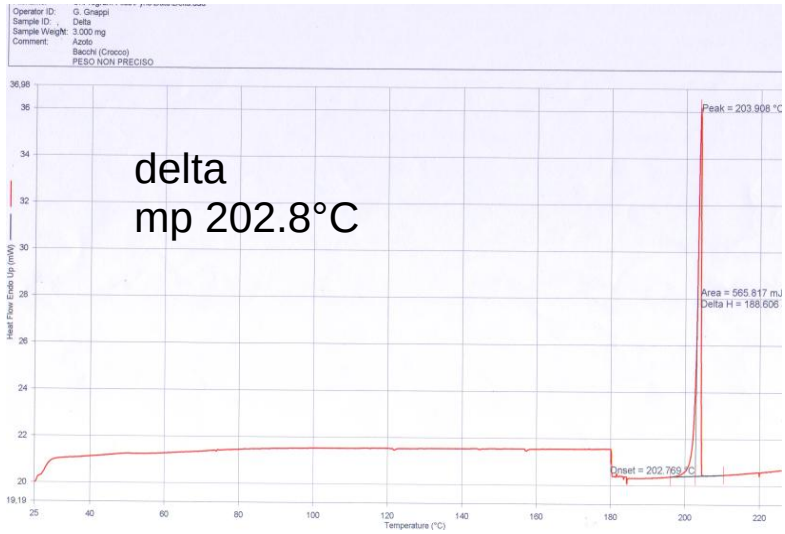

The DSC of the commercial alpha phase was recorded also at 1°C/min and 20°C/min to detect any possible phase transition prior to melting, with no evidence of such a phenomenum.

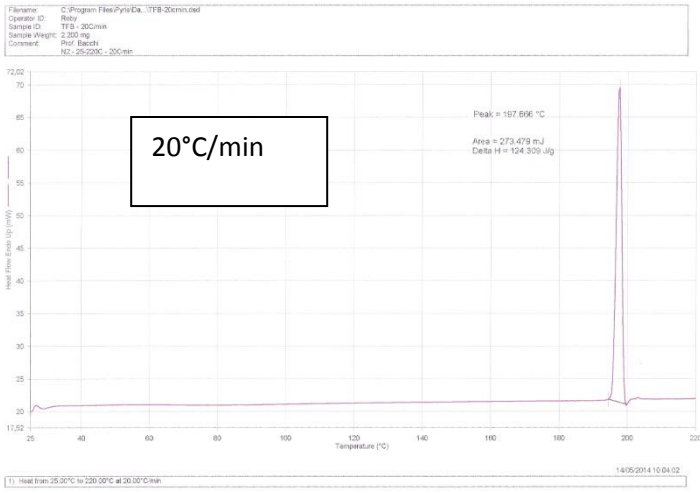

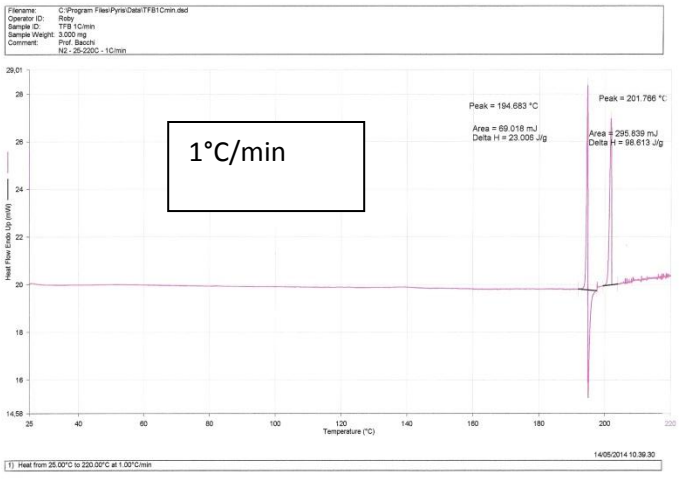

Figure S4. Variable Temperature Raman spectra for thermal treatement of gamma polymorph heated to 170°C and cooled down to RT, showing the transformation gamma→ alpha on cooling.

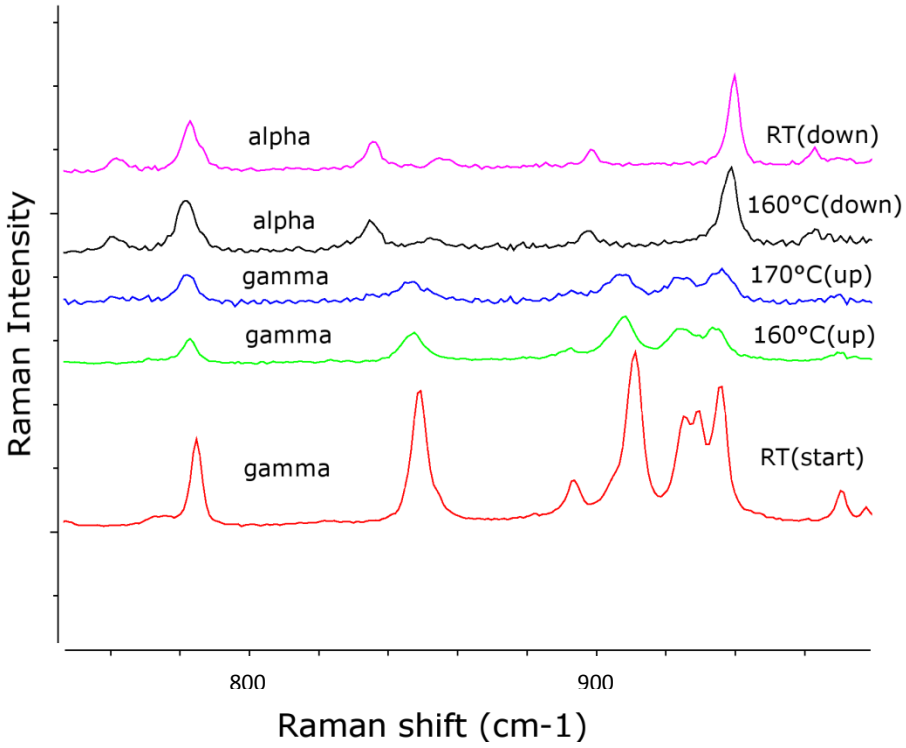

Figure S5. Plot of ΔG for the three possible phase transitions alpha>delta, alpha>gamma and delta>gamma as a function of temperature

$$\Delta G_{A \rightarrow B} = (\Delta H_{Am} - \Delta H_{Bm}) - T(\Delta S_{Am} - \Delta S_{Bm})$$

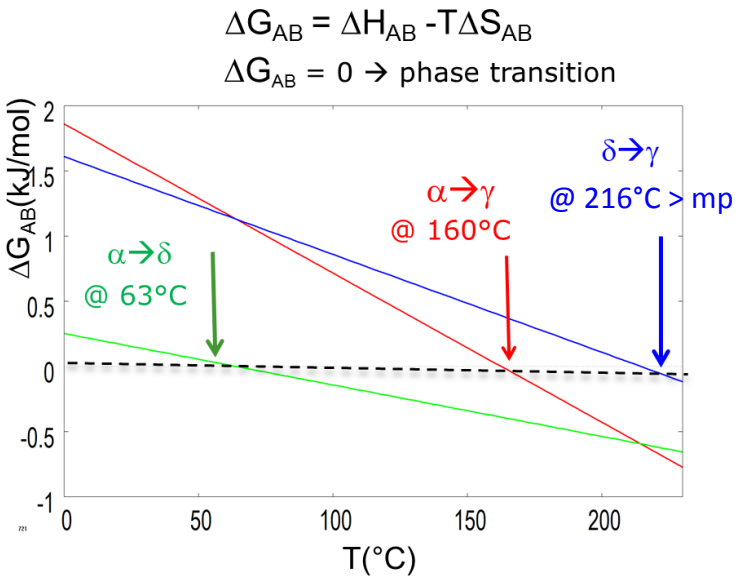

Figure S6. Face indexing of a crystal of alpha-TPB. In pink the shortest intermolecular contact is evidenced.

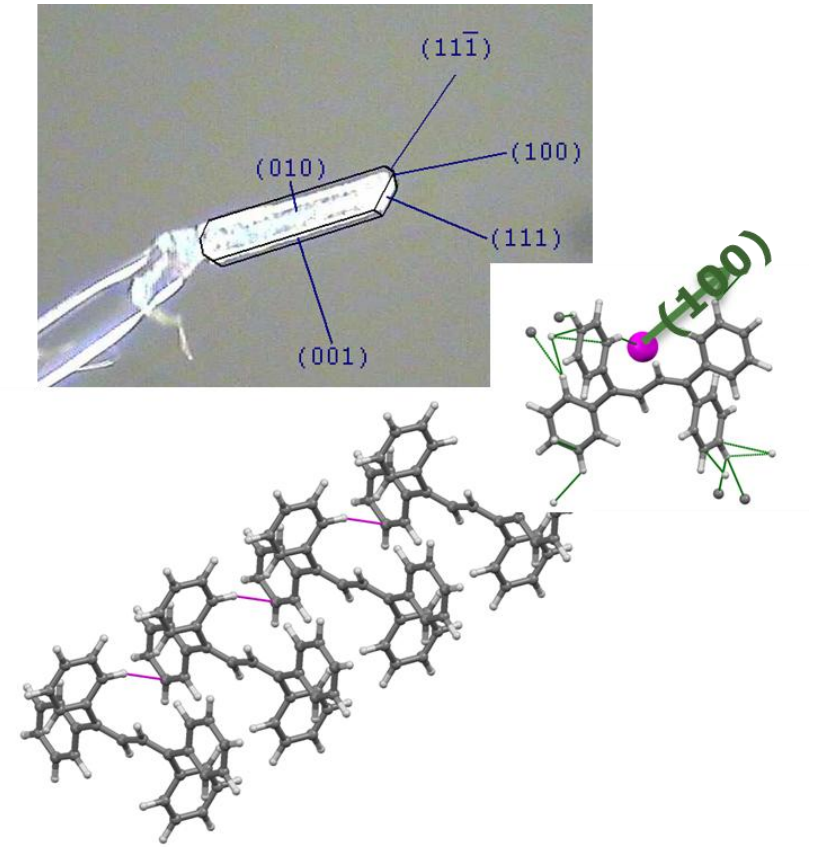

Figure S7 IR spectra of TPB.c-hex freshly prepared (**a**), and after 15 min of exposition of the powder to vapour of ciclohexanone (**b**); the ketone peak is present at 1709 cm^{-1}.

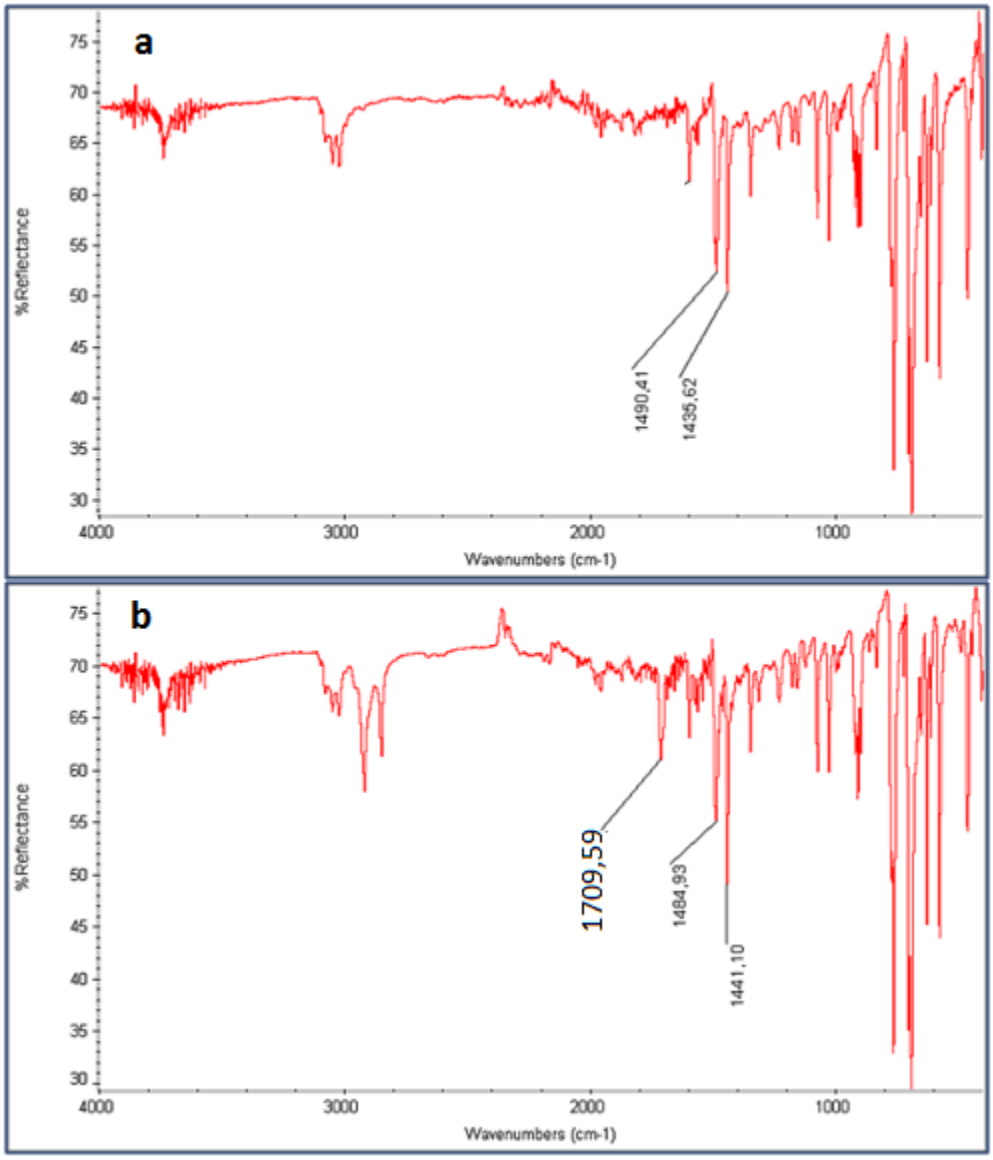

Figure S8. Example of a bent crystal of alpha-TPB, constituting roughly 30% of the commercial product and of recrystallized batches.

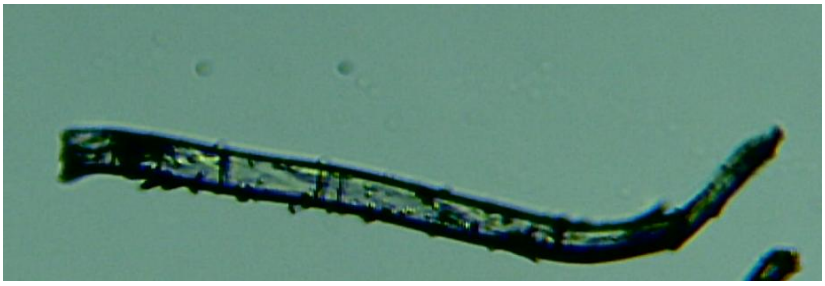

Figure S9. X-ray Powder Diffraction traces of commercial alpha-TPB, with superimposed the calculated trace of the alpha and the delta forms. No detctable traces of impurities are visible.

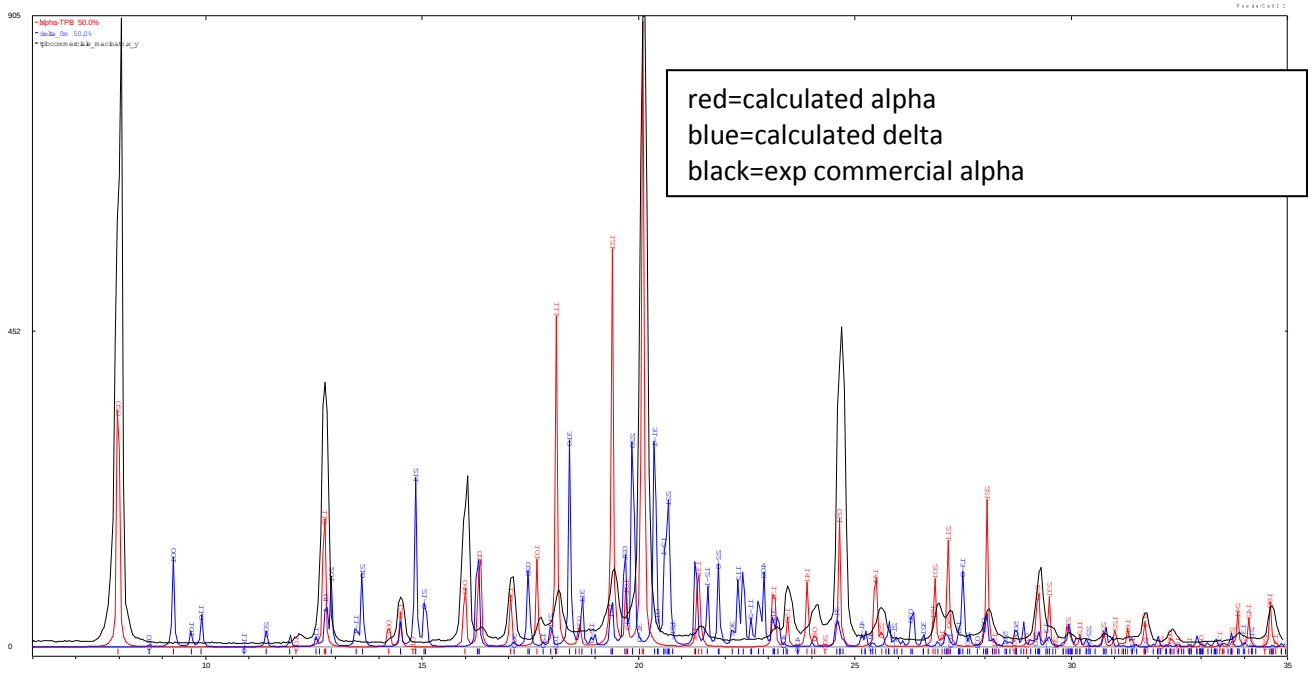

Figure S10. XRPD of the commercial alpha TPB at room temperature, and after 3 hours at 140°C. No phase transition is detected. Peak shift is due to thermal expansion.

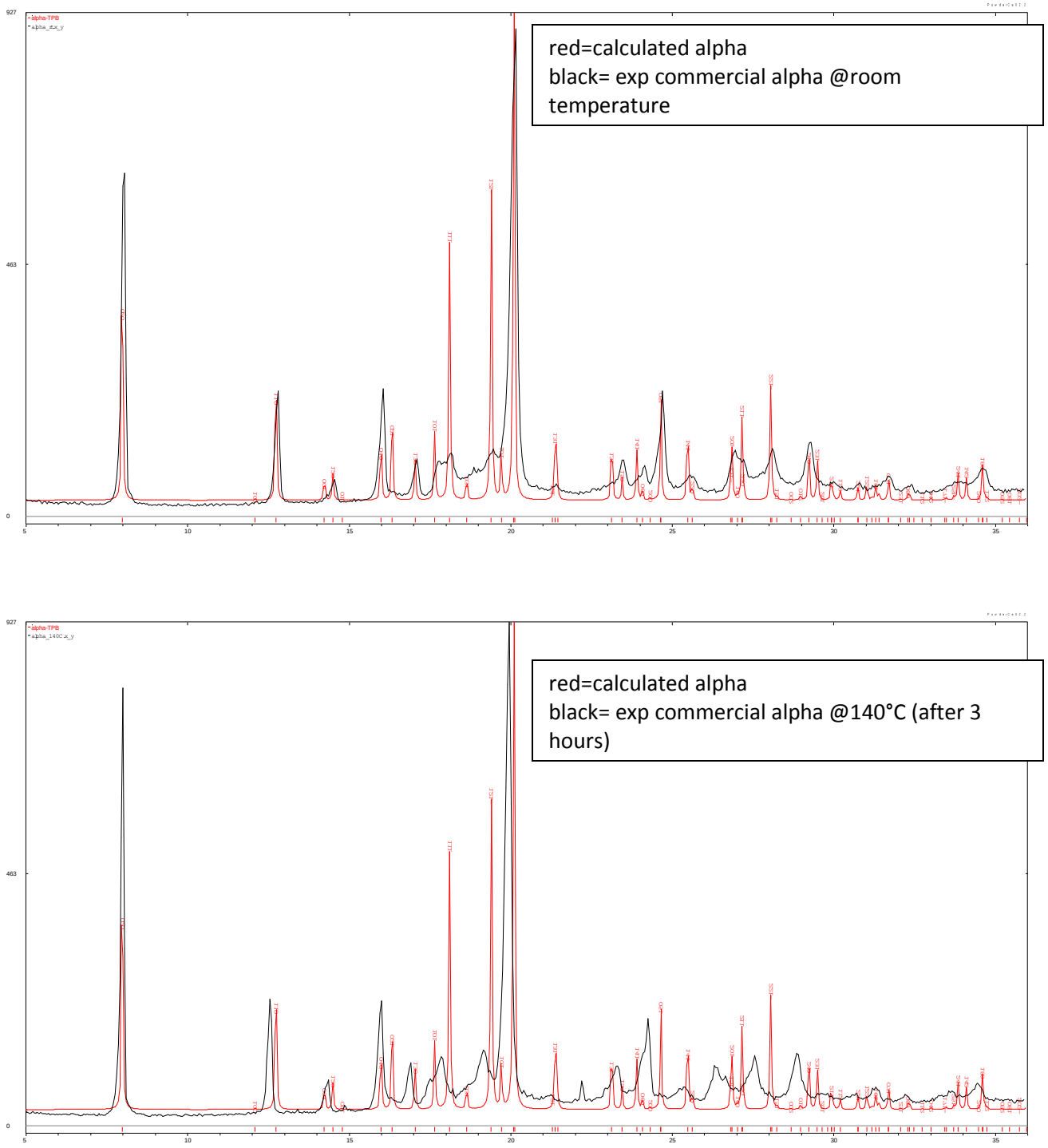

Figure S11. 1H NMR spectra of TPB at different dilution and conditions to investigate molecular aggregation.

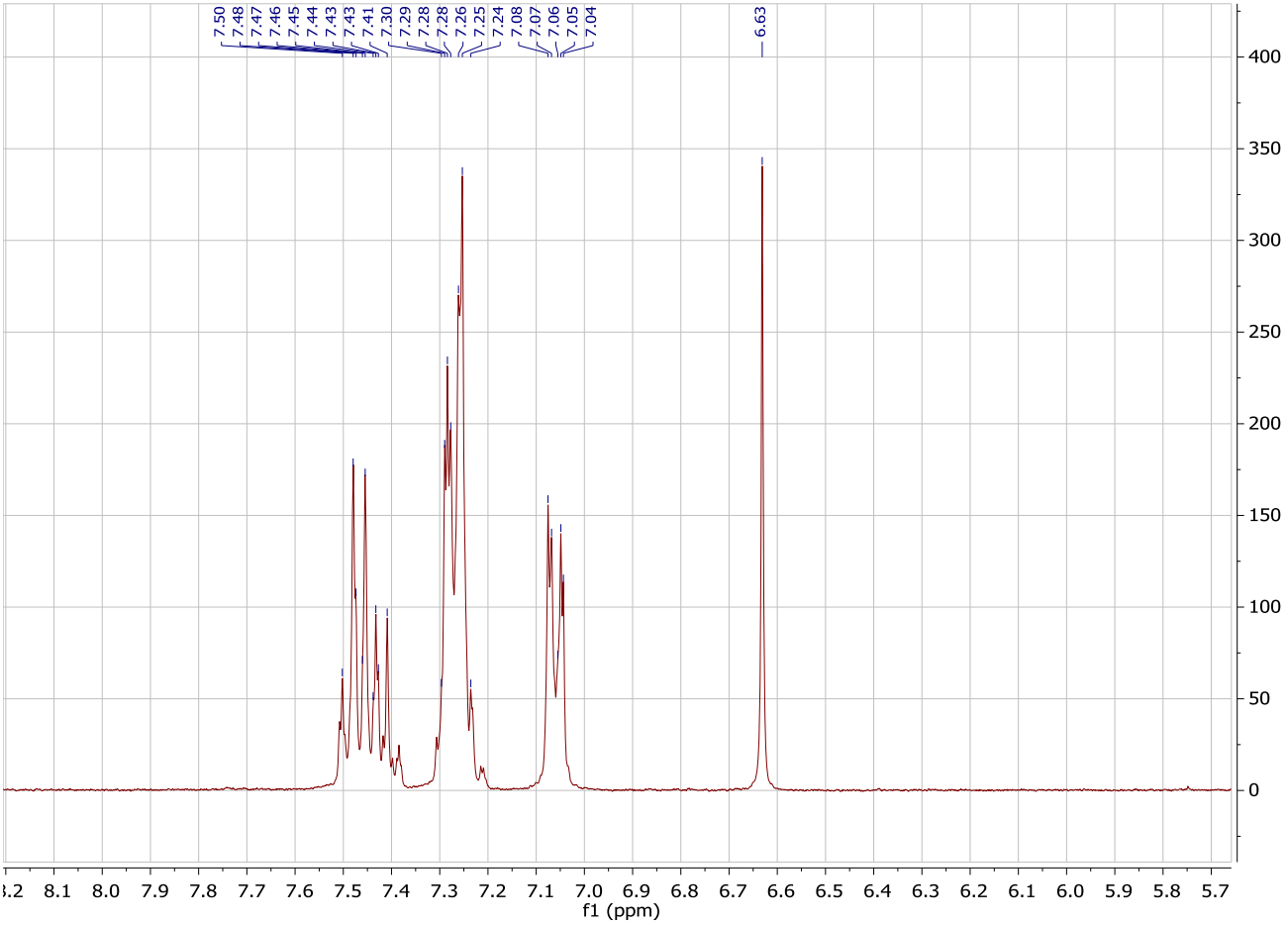

Aromatic region of the ^{1}H NMR spectrum of TPB in dmso-d^{6} (50 mM)

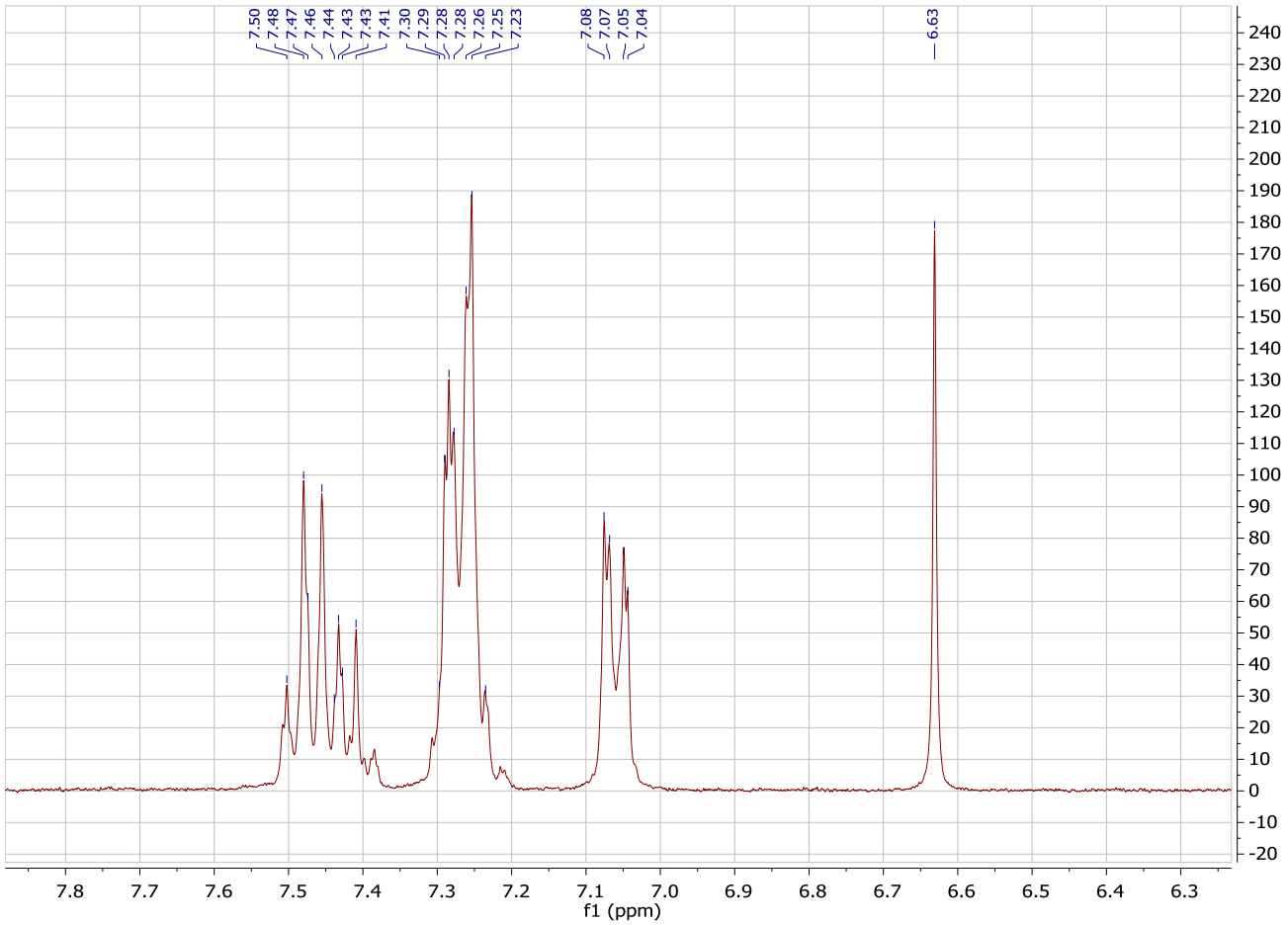

Aromatic region of the ^{1}H NMR spectrum of TPB in dmso-d^{6} (5 mM)